Composites Science and Technology 137 (2016) 35–43

Contents lists available at ScienceDirect

Composites Science and Technology

journal homepage: http://www.elsevier.com/locate/compscitech

Multilevel composite using carbon nanotube fibers (CNTF)

XiaoMeng Sui [a, **, 1], Israel Greenfeld [a, *, 1], Hagai Cohen [b], XiaoHua Zhang [c], QingWen Li [c], H. Daniel Wagner [a, ***]

[a] Department of Materials and Interfaces, Weizmann Institute of Science, Rehovot 76100, Israel
[b] Chemical Research Support, Weizmann Institute of Science, Rehovot 76100, Israel
[c] Suzhou Institute of Nano-Tech and Nano-Bionics, Suzhou 215123, China

ARTICLE INFO

Article history:
Received 15 June 2016
Received in revised form
20 September 2016
Accepted 15 October 2016
Available online 19 October 2016

Keywords:
Carbon nanotube fiber
Nano composite
Fragmentation
Interface
Interphase

ABSTRACT

Multilevel hierarchical structures built up from nanoscale to macroscale are common in nature, but their potential has not been achieved by man-made composites. The presented multilevel structure consists of carbon nanotube fibers (CNTFs) embedded in epoxy matrix. This structure exploits the supreme mechanical properties of individual CNTs together with the manageability of the microscale CNTFs, and has the potential to overcome the implementation difficulties associated with nanocomposites. Using different chemical treatments (ethylene glycol or nitric acid solvents), the CNTFs are densified and the amount of epoxy penetration inside the CNTFs is controlled, creating an interphase between the single CNTs. The strength and adhesion properties of individual CNTFs in epoxy are measured by continuously monitored fragmentation tests and characterized by electron microscopy. A modified Cottrell-Kelly-Tyson model is applied to account for the CNTF unique cross-sectional geometry, comprising millions of individual multiwalled CNTs, and for the effect of matrix penetration. The composite strength and toughness are found to be strongly dependent on and improved by the extent of penetration, suggesting that the composite mechanical properties would be tunable by controlling the interphase. The presented integrative analysis shows that CNTF based composites are an excellent potential choice for strong and tough structures, as well as for bio-engineering.

1. Introduction

Structures common in nature are often multilevel and hierarchical, tuned to the desired functionality at a minimal cost in resources. For example, bone structure is a self-assembled, seven levels composite, which evolved to achieve a balance between toughness and stiffness at a low weight [1]. A natural surface can be adhesive as in the attachment pads on a gecko's foot [2], or repellent as in a lotus leave [3], as a result of different structural hierarchies. Attempts at bio-inspired synthetic composites have not been successful so far, and the performance and efficiency of such composites are far behind their natural counterparts or theoretical prediction. The application of nanocomponents such as carbon nanotubes (CNTs) [4] as reinforcing materials is still limited to lab scale, mainly due to technical obstacles related to their dispersion and alignment in matrices and to their matrix interface [5].

Recently, a new reinforcing component has been proposed in parallel by several groups, exploiting fibers that consist of millions of bundled CNTs (Fig. 1) [6]. These CNT fibers, or CNTFs, are produced by spinning CNTs either from a CNT aerogel [7], or from a CVD-grown CNT array [8], or by coagulation of a CNT-containing polymer solution [9]. Because of the tension and shear forces induced by pulling, twisting and extrusion, the CNTs are well aligned and tightly packed within the CNTF. In addition to high loading (100% CNTs), better alignment, infinite length, and easy handling, CNTFs are flexible, reliable fibers with mechanical and electrical properties that can be tuned by production conditions [10,11]. CNTFs have a compact twisted yarn-like hierarchical structure, spanning across multiple length scales from nanoscale to micro- and macroscale [6,12,13]. The mechanical, electrical and thermal properties of CNTF based composites are affected by the CNTF densification and polymer impregnation [13–15]. These unique structural features allow CNTFs to be a potentially

* Corresponding author.
** Corresponding author.
*** Corresponding author.
E-mail addresses: xiaomeng.sui@weizmann.ac.il (X.M. Sui), green_is@netvision.net.il (I. Greenfeld), Daniel.Wagner@weizmann.ac.il (H.D. Wagner).
[1] These authors contributed equally to this work.

http://dx.doi.org/10.1016/j.compscitech.2016.10.011
0266-3538/

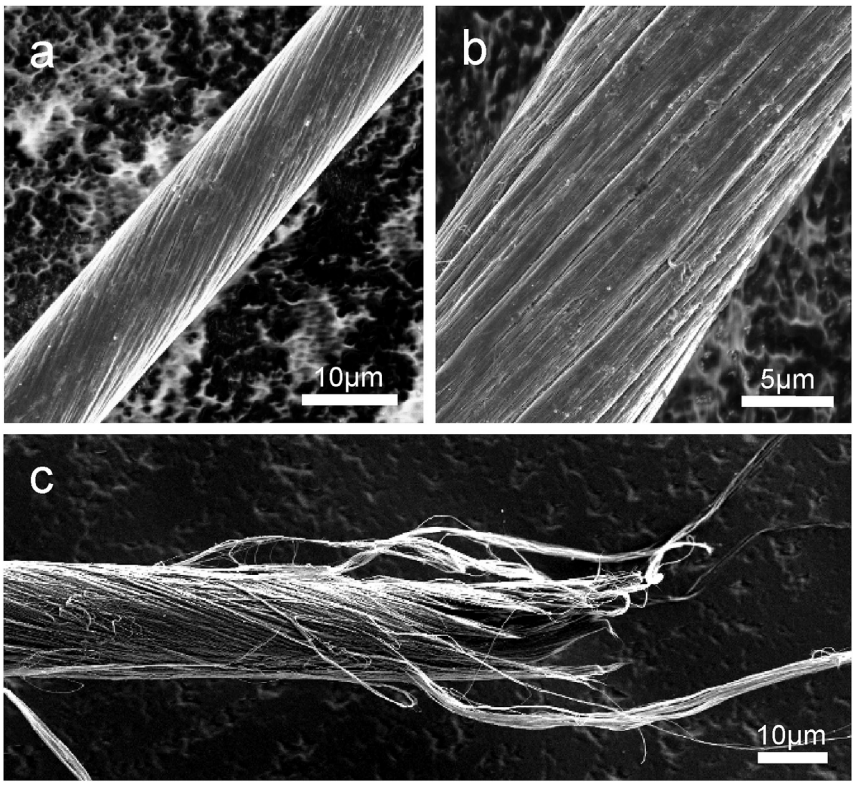

Fig. 1. SEM images of EG-treated CNTFs. (a) As produced. (b) Higher magnification showing the presence of bundles of CNTs in the CNTF. (c) After breaking under tension.

advantageous alternative to traditional reinforcing materials such as carbon or glass fibers, as well as to randomly dispersed CNTs.

Here, we present a four-level composite structure reinforced with CNTFs, which combines the high mechanical properties of CNTs with the flexible structural design enabled by CNTFs. Our focus in the current study is on the effects of the interphase - the matrix medium created by polymer penetration inside the CNTF - on the structural stiffness, strength and toughness. Specifically, the amount of interphase is controlled by applying different surface treatments to the CNTFs prior to their embedding in an epoxy matrix. As a reference, the strength and stiffness of free (in air, without epoxy) as-spun and treated CNTFs under tension are measured. A continuously monitored fragmentation test [16–18] is subsequently used to investigate the strength of embedded CNTFs, as well as the shear strength of the CNTF-epoxy interface. The effects of the chemical treatments are demonstrated and compared, and a Cottrell-Kelly-Tyson (CKT) model [19] is used in a modified form to account for the complex CNTF and interphase geometry. Finally, we expand on the concept of a four-level composite and provide a preliminary analysis on its projected performance.

2. Experimental section

2.1. Materials

The CNTFs used in this work were dry-spun from CVD-grown CNT arrays, as described in previous publications [20,21]. The level of crystallinity was assessed by the ratio of the Raman G and D intensities, I_G/I_D, which was higher than 1.27 [22]. Due to the enhanced bonding between the wafer's buffer layer and the catalyst, there were no catalytic Fe nanoparticles inside the spun fibers [23]. During fiber spinning, ethylene glycol (EG) solvent was used to densify the fibers, and the resulting CNTF is denoted as CNTF(EG). For the nitric acid (HNO_3) treatment, the fiber was first spun from a CNT array, with ethanol applied simultaneously for densification. After being collected, the fibers were immersed in concentrated HNO_3 (16 M) for several hours, washed by water, and finally dried under ambient conditions. HNO_3 is believed to have two functions, *i.e.* to further densify the CNTF and to oxidize the CNTs [21]. Epoxy DGEBA (EP-501P) and curing agent polyetheramine EPC304 were provided by Polymer-Gvulot Ltd. Israel. The mixing ratio was 70:30 by weight.

2.2. Sample preparation

A CNTF was mounted on a dog-bone shaped silicon mold along its axis. Grooves were made on both sides of the mold, so that the CNTF could be centered both vertically and horizontally in the epoxy. A fishing lead bead (about 0.5 g) was attached to each end of the fiber to stretch and preload it. The epoxy and hardener were mixed thoroughly according to the specified ratio, followed by 30 min degassing. The mixture was cast into the mold (with a pre-aligned CNTF), and degassed for another 30 min. Then the epoxy was cured at 100 °C for 6 h. The resulting dog-bone sample had a total length of 30 mm and a gauge length of 12 mm, with width and thickness of about 1.5 mm and 1 mm, respectively.

2.3. Fragmentation test

The continuously monitored single-fiber fragmentation tests were performed on a Minimat tensile tester equipped with a 200 N load cell, with deformation speed at 0.05 mm/min. The tensile tester was mounted on a microscope equipped with polarized light. The experiment was recorded by a CCD camera attached to the microscope for later analysis, with the lens field of view covering the central part of the specimen. The video and the test were

synchronized, so that the stress level of the matrix could be known when fiber breaks happen. Upon saturation (about 60 breaks in each sample), the total number of breaks of the whole fiber was counted by scanning the fiber. See Supporting Information section S1 and CNTF fragmentation video.

2.4. Characterization

Tensile tests were performed for the matrix and each type of CNTF. The gauge length for the tensile sample was 15 mm, and at least 10 samples were tested, for statistical significance. The tensile tests were carried out on an Instron (4502) equipped with a 10 N load cell, and the stretching speed was 1 mm/min. The fiber and fracture surfaces after a fragmentation test were probed by scanning electron microscopy (SEM) and transmission electron microscopy (TEM). For the TEM measurements, samples were prepared by microtome. With the help of a diamond knife on a Zeiss microtome machine, the sample was first embedded in another epoxy block, and then thin slices (about 100 nm) were cut perpendicular to the fiber/sample axis, close to the fracture end. The thin slices were collected on a Cu grid, which was coated with cellulose film and sputtered with carbon before the collection. The chemical composition of the CNTFs was investigated by X-ray photoelectron spectroscopy (XPS) (Supporting Information section S5), performed on a Kratos AXIS-Ultra DLD spectrometer, using a monochromatic Al kα source at low fluxes, 15–75 W, and detection pass energies of 20–80 eV. The pressure at the analysis chamber was kept below $1 \cdot 10^{-9}$ torr. Stability of the CNTs signals was checked by repeated measurements and found to be remarkably good.

3. Results and discussion

3.1. CNTF treatments and strength

The CNTFs used in this study were spun from aligned CNT arrays/forests, themselves synthesized by CVD (Fig. 1a). The CNTs are multiwalled with 2–3 graphene layers, with external diameters smaller than 10 nm [22]. During CNTF preparation, chemical treatment was applied, either by spraying ethylene glycol (EG) while spinning the CNTs into a fiber, or by first spraying ethanol then soaking the spun CNTFs in nitric acid (HNO_3). The resulting external CNTF diameters were 14.5 μm (EG-treated) and 7 μm (HNO_3-treated) on average. See Experimental.

Load transfer in CNTs and CNT-epoxy composites arises from micromechanical interlocking, van der Waals bonding, and chemical bonding [24], achieved here through CNTF surface roughness, epoxy penetration, and CNT functionalization. It has been demonstrated that solvent treatment can improve the CNT coherence in a CNTF, leading to a denser CNTF structure [13–15,20,21,25]. EG was found to be the best solvent for densification, whereas HNO_3 is a well established acid for creating functional groups on CNTs [21,26]. The solvents neutralize electric charges gathered on the CNTs during CNTF preparation, thereby reducing the CNTs electrostatic repulsion, and evaporation of the solvents draws the CNTs closer. The bundling of CNTs seen in Figs. 1b and 2d is likely the result of strong local intermolecular forces enhanced by solvent densification. As a result of spinning, chemical treatment, and solvent evaporation, the thin bundles inside the CNTF (Fig. 2d) seem to coagulate into bundles about an order of magnitude larger on the CNTF boundary (Fig. 1b). Similar graded bundling morphology is described in the review by Espinosa et al. [12].

Since the CNTF(HNO_3) sample was condensed in two steps, its structure is denser than that of the EG treated sample. These effects enhance the contact between CNTs, and consequently increase the inter-CNT adhesion and the overall stress transfer in a CNTF cross section. The HNO_3 treatment also acidizes the CNTs and forms carboxyl (−COOH) and hydroxyl (−OH) groups on them [21]. These groups react with each other and with the epoxy during composite preparation, and consequently largely prevent the epoxy from penetrating inside the CNTF. X-ray photoelectron spectroscopy (XPS) confirms the chemical difference between these two types of treated CNTF, by identifying the functional groups associated with each treatment (see Supporting Information section S5).

Tensile tests were performed on free untreated and treated CNTFs, as well as on the epoxy matrix (Table 1), to generate reference data prior to the interface measurements. The untreated CNTF has the lowest measured strength (0.48 GPa), followed by the EG treated CNTF (0.75 GPa), and the HNO_3 treated CNTF has the highest measured strength (1.23 GPa), results that correlate well with the degree of densification. Higher densification increases the CNTF material density, and is expected to improve stress sharing in a CNTF cross section, and to screen out some of the critical defects by bridging. Although functionalization (by HNO_3) may decrease the strength, as it breaks CNT's carbon-carbon bonds [27], densification remains the dominant effect.

Fracture of a free CNTF under tension (Fig. 1c) reveals a “brush-like” aspect at different positions along the CNTF, a fracture pattern familiar in Kevlar fibers (and in macroscale ropes and steel cables), though at a scale 2-3 orders of magnitude smaller. The reason for this pattern is the stochastic occurrence of weak points and critical defects along bundles (“weakest links”), which, in the absence of interface with a matrix, determine the location of break in each bundle. The stress-strain curves are non-linear, with increasing modulus as the load in increased, and the fracture is brittle, without yield. Also notable is the fact that the CNT bundles seem to remain compact after fracture, implying a very strong internal adhesion. By contrast, the fracture surface in CNTFs embedded in a matrix, particularly when an interphase is present (Fig. 2a), is nearly planar, in other words bundle failure occurs close to the fracture plane rather than at the weakest link of each bundle. In this way the effect of fiber defects is mitigated (*i.e.,* the weakest links are avoided).

3.2. CNTF in epoxy - interfacial strength

The treated CNTFs were embedded in epoxy, a single CNTF in each dog-bone shaped sample (see Experimental), as preparation for fragmentation tests. Vacuum was applied to the specimen for 30 min before increasing the temperature, for the purpose of degassing and to enhance polymer penetration into the CNTF. Since the epoxy used (EP501p) has high viscosity (110-150 P at 25 °C) [28], it has low penetration capability. Accordingly, we observed minimal penetration inside the highly densified HNO_3 treated CNTF (Fig. 2g), and higher penetration throughout the CNTF cross section in the less densified EG treated CNTF (Fig. 2c). Penetration could possibly be tuned by controlling the degassing time and curing temperature, but these are subject to the epoxy handling time. For example, increasing the temperature will enhance the penetration rate owing to lower viscosity, but at the same time the curing process will be accelerated and the penetration time cut short.

An additional likely effect is the reaction of the carboxyl and hydroxyl groups, created by the HNO_3 treatment on the CNTF surface, with the amine groups in the epoxy hardener, forming sparse covalent bonds between the surface of the CNTF and the epoxy. Due to the high density of the HNO_3 treated CNTF, the covalent interaction is more likely to occur only at the CNTF boundary, and to have a lesser interfacial effect compared to the augmented bonding area in the EG treated CNTF.

To investigate the mechanical consequences of the different treatments on the CNTF-matrix interface, a continuously monitored

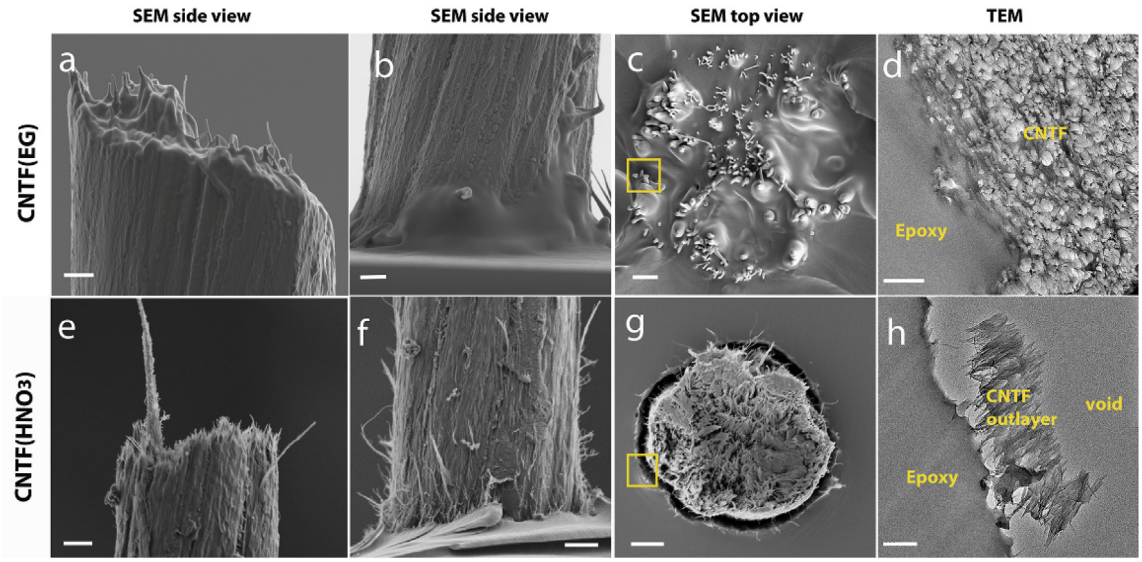

Fig. 2. SEM and TEM images of CNTFs in epoxy after breaking. The SEM images are of the fracture surfaces without any further treatment (except for sputtering). The TEM images were taken from microtome slices close to the fracture surface, and are magnifications of the corresponding SEM regions marked by yellow squares. The scale bars are 2 μm in a-c and e-g, 500 nm in d, and 200 nm in h. (For interpretation of the references to colour in this figure legend, the reader is referred to the web version of this article.)

Table 1
Tensile test results of epoxy and free CNTFs with and without treatment.

	E^a [GPa]	$\sigma_f{}^a$ [MPa]	ε [%]	Weibull distribution[b]	
				α [MPa]	β
Epoxy	0.7 ± 0.1	46.7 ± 3.3	17.9 ± 4.0	48.3	15.5
CNTF	28	480	9–10	–	–
CNTF(EG)	33.9 ± 5.4	753.7 ± 47.5	2.3 ± 0.4	774.6	18.8
CNTF(HNO_3)	46.1 ± 6.1	1233.1 ± 179.4	2.6 ± 0.2	1312.0	8.7

[a] The CNTFs Young's modulus and strength were calculated for the total CNTF cross-sectional area including voids.

[b] The strength of each sample was fitted to a two-parameter Weibull distribution, *i.e.* $F(\sigma_f)=1-\exp[-(\sigma_f/\alpha)^{\beta}]$, where $F(\sigma_f)$ is the probability of failure, α is the scale parameter, and β is the dimensionless shape parameter.

fragmentation test was performed (see Experimental). In such a test both types of treated CNTF gradually broke at various arbitrary axial positions due to the stress transferred via the interface, until the fragmentation process, and the break density, reached saturation. The epoxy resin chosen in this work has a much longer elongation than the densified CNTFs, ensuring efficient transfer of the interfacial shear stress throughout the test and process saturation. The profile of the matrix shear stress upon fiber fragmentation can be visualized under polarized light (Fig. 3, and CNTF fragmentation video in Supporting Information). The enhanced stress field in the matrix is seen in the image as a symmetrical, butterfly-shaped birefringent pattern around the CNTF broken edges, with a high stress at fragments ends. The fragmentation test was continuously monitored and recorded, enabling simultaneous measurement of the fragments length and the fiber strength upon each break.

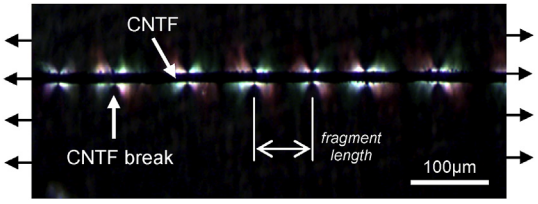

Fig. 3. Fragmentation pattern of a CNTF in epoxy under tension. Birefringence image under an optical microscope equipped with polarized light, showing the regions where the epoxy is more highly stressed (in color). Near the fragment edge (*i.e.,* CNTF break), the very bright color indicates high shear deformation and stress in the matrix, as a result of the large mismatch in stiffness between the fiber and the matrix. (For interpretation of the references to colour in this figure legend, the reader is referred to the web version of this article.)

Supplementary video related to this article can be found at http://dx.doi.org/10.1016/j.compscitech.2016.10.011.

For data analysis, we used the classic Cottrell-Kelly-Tyson (CKT) model [29,30]:

$$\tau = \frac{\sigma_f(l_c)D}{2l_c} \quad (1)$$

in which τ is the effective interfacial shear strength, D is the fiber diameter, and l_c is the fiber critical length derived from the average fragmentation length at saturation. The critical length is the fiber length below which the stress transferred to the fiber via the matrix is not sufficient to further break it. $\sigma_f(l_c)$ is the effective strength of a fiber with length equal to the critical length, and one of the reasons for using the continuously monitored fragmentation test [16–18] is that it is easy to obtain a good approximation for $\sigma_f(l_c)$. The calculated interfacial and fiber strengths are effective (or apparent) rather than actual (or intrinsic, independent of CNTF geometry), remembering that equation (1) is valid for a circular solid fiber and not for a CNTF that contains voids and penetrated polymer. This issue is clarified in depth in the modified CKT model section.

The results of the fragmentation tests are summarized in Table 2, including the critical lengths, CNTF strengths with their Weibull distribution parameters, and interfacial strengths. As seen in the table, the critical lengths for CNTF(EG) and CNTF(HNO_3) are similar, ~270 μm and ~310 μm, respectively. Since the strength and toughness of a composite depend predominantly on the filler's critical length (Supporting Information section S4), should these fibers be embedded in a matrix with the same volume fraction, the composite strength and toughness would be similar.

The calculated effective interfacial strength in the CNTF(EG) is much higher than in the CNTF(HNO_3), 74 MPa compared to 41 MPa, respectively. This is the likely consequence of the augmented

Table 2
Fragmentation test results of densified CNTFs in epoxy.

	D[a] [μm]	l_c [μm]	Weibull distribution[b]		σ_f[c] [GPa]	τ[c] [MPa]
			α[d] [GPa]	β[d]		
CNTF(EG)-Epoxy	14.5	268.8 ± 34.2	2.6 ± 0.5	22.1 ± 11.9	2.7 ± 0.5	73.9 ± 13.2
CNTF(HNO_3)-Epoxy	7.0	306.8 ± 46.1	3.4 ± 0.2	32.8 ± 7.6	3.5 ± 0.2	40.6 ± 4.8

[a] The diameter variations over a 2 cm fiber length were less than 5%.
[b] The Weibull distribution parameters were calculated by equation (S1) in Supporting Information section S1.
[c] Effective (i.e., apparent) strength.
[d] The data sets of the EG and HNO_3 treated samples are significantly different from each other (t $test_\alpha = 0.0005$ and t $test_\beta = 0.05$).

matrix-fiber contact area in the CNTF(EG), owing to the matrix penetration into the CNTF. By comparison, the interfacial strength measured by Chou's group in their pioneering work, using micro-droplet tests [31] and fragmentation tests [32], was below 20 MPa, comparable to traditional E-glass-epoxy and carbon-epoxy. However, the fibers tested in Chou's experiments were not treated, and the samples not degassed, an important factor in increasing polymer penetration and consequently the effective interfacial strength. This is a convincing demonstration of the tuning flexibility with CNTFs, made possible by different treatments and processing, which, as discussed later, is an important feature when searching to achieve a tradeoff between strength and toughness. Low interfacial strength usually increases the critical length, and is therefore advantageous for toughness because more energy is dissipated by the friction between the fiber and matrix. On the other hand, high interfacial strength decreases the critical length, and enables exploitation of the fiber to its utmost strength.

3.3. CNTF in epoxy – fiber strength

The continuously monitored fragmentation test can also provide statistical information on the effective fiber strength (*i.e.*, assuming a solid circular fiber). To that end, the strength and length of the fiber fragments, as they gradually broke, were fitted to a two parameter Weibull distribution (see Supporting Information section S1), and the distribution's scale and shape parameters derived (Table 2). The strength distributions of free and embedded CNTFs are compared in Fig. 4.

The improvement in strength from free to embedded

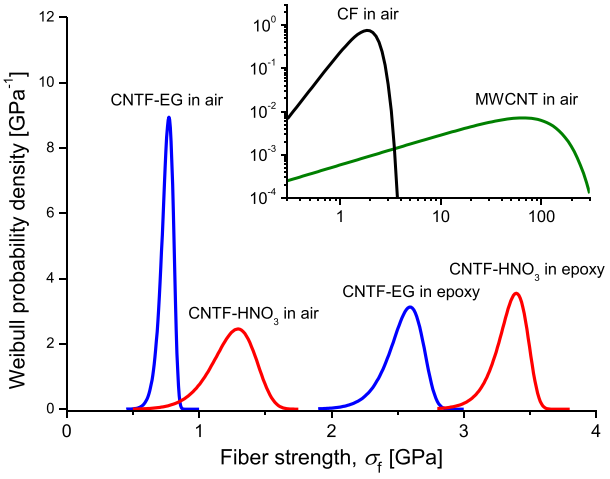

Fig. 4. Weibull strength distributions of CNTFs in air and in epoxy. The Weibull scale (α) and shape (β) parameters used in these density functions are the average measured values from Tables 1 and 2, calculated by the standard CKT model prior to its adjustment. The log-log plot (inset) compares these results to an individual MWCNT [33] and carbon fiber (CF) [34].

configuration is significant, approximately by a factor of three (from 0.8 GPa to 2.7 GPa for CNTF(EG), and from 1.2 GPa to 3.5 GPa for CNTF(HNO_3)). As reasoned before, when the CNTF is in epoxy, the composite failure is confined to the highly-stressed fracture plane, and consequently CNT defects are mitigated (clarified later). This improvement is comparatively larger for the HNO_3 treated fiber (distance between peaks of the same color), possibly due to mitigation of treatment-induced CNT defects. Furthermore, it is seen that the strength of the HNO_3 treated fiber is significantly higher than that of the EG treated fiber, for both the free and embedded configurations. This is attributed to the higher compactness of the CNTF(HNO_3) and to the added bonding due to functionalization, resulting in better stress transfer between the bundled CNTs.

The measured values of the shape parameter (β) for the CNTFs in epoxy are much higher than those of untreated CNTFs and traditional fibers [32], indicating a much lower (better) statistical variability of the strength. In our case, the values of β were 22.1 and 32.8 for CNTF(EG) and CNTF(HNO_3), respectively (Table 2 and Fig. 4). Similarly, the corresponding values for the free CNTFs were 18.8 and 8.7. Note that the latter values were also higher than those of untreated CNTFs reported in the literature [32]. This is the consequence of densification, which enhances the adhesion between the CNTs due to higher van der Waals interaction and friction forces, and improves the stress transfer between individual CNTs or CNT bundles, eventually resulting in more uniform load sharing within the CNTF. These exceptionally high β values, obtained for the first time for CNTFs embedded in a matrix, are surprising and promising, and merit further investigation and validation.

The advantage of a structure comprising millions of bundled CNTs is even more striking when noting that for a single CNT the typical value of β is much lower, of the order of 1.7 [33], and for a CF (carbon fiber) the value is of the order of 3–5 [34] (Fig. 4(inset)). Although CNTFs and CFs have comparable strengths, the advantage of a CNTF is expressed in its lower mass density (about half that of a CF), and in its smaller strength variability. Clearly, the bundling of CNTs into a CNTF decreases the strength variability at the expense of the mean strength (Fig. 4(inset)), but the higher strength of individual CNTs sets the bar for potential future improvement of the CNTF strength. The calculated dispersion (std) of the embedded CNTF strengths is less than 1% of the mean strength, a value that is quite practical for engineering applications. This means that, in a given experimental sample, the local strength at different positions along the CNTF is quite uniform, indicating a stable fiber strength.

3.4. CNTF in epoxy – fracture behavior

The EG treated CNTF shows significantly higher effective interfacial shear strength compared to the HNO_3 treated CNTF, although both types of CNTFs are based on the same CVD-grown CNT array and are embedded in the same matrix. Study of the fracture surfaces of both CNTFs after the fragmentation tests, carried out under electron microscopes, reveals conformational differences between the two structures, and helps clarify the observed difference in

shear strength (Fig. 2).

Epoxy clearly infiltrates the CNTF(EG) structure and fills its inner voids, enclosing the CNT bundles (Fig. 2a and c). In some of the samples, the CNTF(EG) pulled out as a whole from the epoxy matrix during failure, leaving a smooth surface on the fiber protrusion (Fig. 2b). Magnification by TEM shows that the fiber part still embedded in the matrix remains in good contact with it, and its boundary blends with it (Fig. 2d). The interface failure is characteristic of a plastic failure of a ductile matrix, as it yields under the high interfacial stress and flows plastically. These observations confirm that epoxy has substantially penetrated the CNTF(EG) structure, thereby producing an "interphase region" between CNT bundles inside the CNTF. That epoxy region seems to be uniformly distributed within the CNTF, and in good structural integrity with the matrix outside the CNTF. In other words, the CNTF(EG) with its internal interphase can be regarded as a distinct structural level of the composite, which, at the higher level, may serve as the reinforcing filler of the composite.

By contrast, the CNTF(HNO_3) structure is barely penetrated by epoxy (Fig. 2e and g). The fracture surface of the CNTF(HNO_3) is hairy (Fig. 2f), and the CNTF appears to have debonded from the surrounding epoxy upon composite failure (Fig. 2g), with torn off CNT bundles left attached to the matrix (Fig. 2f and h). There are no signs of plastic yielding of the matrix at the interface, contrary to the CNTF(EG) case, implying that the interface failure occurred at a stress lower than the matrix yield strength. It can be concluded that, although the functional groups on the fiber surface reacted with the epoxy and formed covalent bonds, the effective interfacial strength was relatively low. Evidently, this is the result of the epoxy not being able to infiltrate the highly dense CNTF, and by that, to increase the overall interfacial area. The fiber in the CNTF(HNO_3)-epoxy structure behaved in a way similar to a regular reinforcing fiber, in the sense that only its outer boundary bonded with the matrix, whereas the fiber in the CNTF(EG)-epoxy structure presented a more complex bi-level interface due to polymer penetration. The interfacial strengths, 41 MPa for CNTF(HNO_3)-epoxy and 74 MPa for CNTF(EG)-epoxy, should be regarded as effective rather than actual values, reflecting the augmented interfacial contact area due to surface roughness and polymer penetration. This distinction between effective and actual strengths is analyzed in more detail in the next section, where we show that effective values are much higher than actual values.

We also observe that in both composite types, the propagation of a crack remains mostly confined to the fracture plane (Fig. 2a and e), in other words, the crack does not wander between arbitrary weak points along the fiber (as in the free CNTF in Fig. 1c). This means that an individual CNT, or a CNT bundle, does not break randomly at weakest points along its length, but at points close to the crack tip where the stress in the composite is maximal. This effect raises the strength of a CNTF embedded in a matrix three-fold compared to a free CNTF, as observed by the measurements (Table 1, Table 2 and Fig. 4). From a fracture mechanics perspective, this means that the energy required to advance a crack increases, and therefore the critical size of a crack is larger in a CNTF embedded in matrix compared to a free CNTF, in other words, it is less sensitive to defects. Equivalently, the critical number of CNTs, or the number of broken CNTs above which the crack will propagate spontaneously, is higher in an embedded CNTF compared to a free CNTF. Key parameters that could influence this fracture behavior are the type of the CNTF-matrix bonding and its strength, and most importantly the size and strength of the interphase, all of which affect crack propagation. Another possibly influencing parameter is CNTF shrinkage under load (Fig. 2 and Supporting Information section S6).

3.5. Modified CKT model

The CKT model in equation (1) ideally assumes a solid fiber with a circular cross section of diameter D, whereas a CNTF is comprised of millions of hollow multiwalled CNTs, and encloses voids between the CNTs in a bundle and between bundles, as well as a possible matrix interphase. Furthermore, the CKT model assumes perfect stress transfer within the fiber, whereas the shear stress transfer between neighboring CNTs or CNT bundles in a CNTF is influenced by gaps and polymer penetration. Hence the traditional CKT model should be adjusted to the structure of a CNTF, with and without an interphase. The theoretical investigation of CNT bundles in our previous work [19] is applied here, taking into consideration the actual complex cross sectional geometry of the CNTF (Fig. 5). We consider two conformations: tight packing (Fig. 5a), representative of a bundle structure, and loose packing (Fig. 5b), representative of a CNTF structure. The details of the revised model are provided in Supporting Information section S3.

Equation (1) can be generalized for an arbitrary cross sectional geometry and interphase size, by defining an effective CNTF diameter $\langle D\rangle$ [19]:

$$\tau = \frac{\sigma_f \left\langle D \right\rangle}{2l_c}, \quad \left\langle D \right\rangle \equiv \frac{4a}{p}, \tag{2}$$

where, σ_f and τ are the CNTF actual tensile and interfacial material strengths, respectively, a is the CNTF material cross-sectional area, and p is the actual CNTF interfacial perimeter (the contact area marked by the thick line in Fig. 5). Introducing a dimensionless geometric factor C_{td} and a dimensionless penetration factor P, the effective CNTF diameter can be expressed by:

$$\langle D\rangle = C_{td}(1-P)D. \tag{3}$$

C_{td} is a function of a tight packing geometry (Supporting Information equation (S14)), and ranges from 0 for a thin wall CNT to ~0.58 for a solid fiber (not tubular). P reflects the amount of matrix penetration in a loose packing geometry (Supporting Information equation (S18)), and ranges from 0 for zero penetration and increases toward 1 for growing penetration, where the limit of 1 is approached when the CNT bundles are completely separated from each other by surrounding matrix.

These concepts are captured in Table 3 and Supporting Information Fig. S1, for the experimental data of this study. The actual tensile strengths are adjusted for the cumulative material

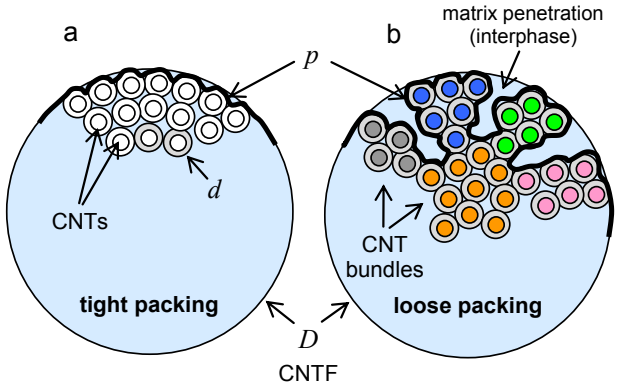

Fig. 5. Illustration of CNTF tight and loose packing. (a) Tightly packed CNTF (hypothetical), consisting of many CNTs. (b) Loosely packed CNTF, consisting of many bundles of CNTs. d is the CNT external diameter, D is the CNTF external diameter, and p is the interfacial perimeter.

Table 3
Results adjusted to modified CKT model. Comparison of σ_f and τ values for CNTF in epoxy, using the standard and modified CKT models, for tight and loose packing.

	Single MWCNT (Literature)[a]	CNTF Standard CKT (Table 2)[b]		CNTF adjusted CKT *tight packing*[b,c]		CNTF adjusted CKT *loose packing*[a,d]	
		EG	HNO_3	EG	HNO_3	EG	HNO_3
σ_f [GPa]	11–150	2.7	3.5	6.5	8.4	6.5	8.4
τ [MPa]	10–90	73.9	40.6	47.0	25.8	23.5	23.3

[a] Actual (*i.e.*, intrinsic) material strength.
[b] Effective (*i.e.*, apparent) strength.
[c] The *tight packing* calculation provides hypothetical values if the CNTs are assumed to be packaged in a tight hexagonal packing.
[d] The *loose packing* calculation assumes a polymer penetration factor of 0.1 (HNO_3) and 0.5 (EG), in general correspondence with the experimental observations.

cross sectional area of the CNTs, by a factor of $(C_{td}\pi/2)^{-1} \cong 2.39$ (Supporting Information equations (S12) and (S14)), given $C_{td} \cong 0.267$ (equation (S16)). The actual interfacial strengths where obtained by equations (2) and (3), where we used $P = 0$ for the hypothetical tight packing, $P = 0.1$ for the HNO_3-treated CNTF where we observed a little penetration, and $P = 0.5$ for the EG-treated CNTF where we observed substantial penetration. Alternatively, the actual interfacial strengths can be obtained by applying a factor of $C_{td}(1-P)/(C_{td}\,\pi/2)$ or $2(1-P)/\pi$ to their respective effective values. The estimated actual interfacial strengths for both solvent treatments are similar, since both are basically a material property of the same matrix. The effective diameters in both treatments are similar, 1.9 μm for the CNTF(EG) and 1.7 μm for the CNTF(HNO_3), and since their material properties are similar, their critical lengths should be similar as well (as indeed measured), even though their external diameters are apart by a factor of more than 2 (Table 2). In the next section, we show how these properties could impact the potential performance of a composite reinforced by the two types of treated CNTF.

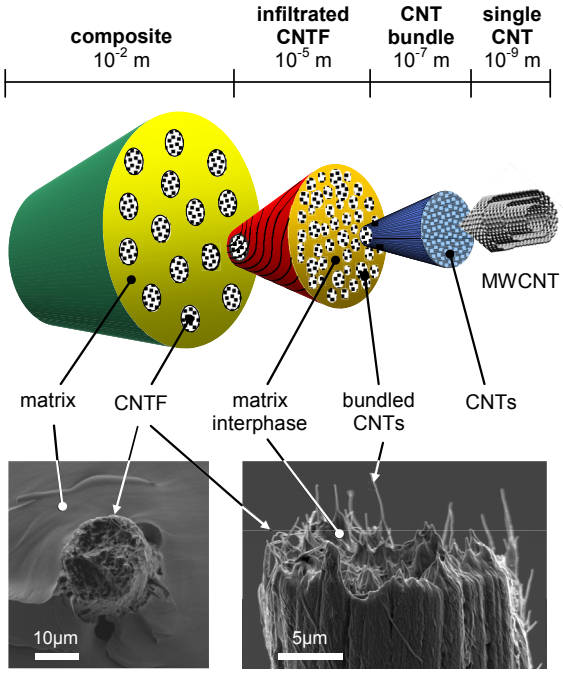

Fig. 6. Illustration of a multilevel hierarchical composite. The composite consists of carbon nanotube fibers (CNTFs) embedded in a matrix. Each CNTF contains numerous bundles of CNTs, surrounded by a matrix interphase. Each bundle contains thousands of densified individual CNTs. The diametric scale of each hierarchical level is denoted. The SEM images show a single CNTF embedded in epoxy and penetrated by it.

3.6. A multilevel composite using CNTFs

The presented composite has four levels (Fig. 6): individual CNTs, CNT bundles (matrix never penetrates here), CNTFs (with or without matrix penetration), and composite (CNTFs surrounded by matrix). The strong intermolecular adhesion between the unidirectional CNTs encourages the creation of CNT bundles (Figs. 1b and 2d), each containing ~10^3 tightly packed CNTs at a cross section. The CNT bundles are loosely packed within the CNTF, ~10^3-10^4 at a cross section, amounting to a total of ~10^6-10^7 CNTs. The matrix is allowed to penetrate (impregnate) the gaps between the bundles (but not inside the bundles, also mentioned in literature [13,14]) during composite preparation, creating the interphase. The amount of matrix penetration, or, in other words, the size of the interphase, as well as the bundles diameter, depend on the CNTF densification by chemical treatment (described before).

This multilevel hierarchical structure bears resemblance to the structure of a tendon (6 levels: tropo-collagen, micro-fibril, sub-fibril, fibril, fascicle, and tendon [35]), and can be similarly optimized. The key to such optimization is being able to control the type and size of the matrix interphase embedded inside the CNTF. Generally, the higher the CNT content in a composite, the higher its strength and stiffness. Yet, the presence of a small amount of soft matrix around and inside a CNTF is essential for toughness, as this medium arrests and diverts crack propagation, and absorbs fracture energy. This tradeoff is revealed in bone structure, where the elementary structural unit consists of a very high fraction of hard carbonated apatite platelets embedded in soft collagen bundles [1,36], providing a balance between strength, stiffness and toughness at a minimal weight. Furthermore, such 2D confinement of the matrix in-between filler elements is tougher compared to unconfined 3D matrix.

Although a detailed theoretical analysis of the multilevel structure is beyond the scope of this study (see example of an early analysis in Akiva et al. [36]), some of the performance trends may be identified. Generally, the ratio between the filler-matrix interfacial area ($\sim DL$) and the volume of the matrix trapped between the fillers ($\sim D^2L$) is inversely proportional to the diameter of the filler ($\sim D^{-1}$), whether a complete CNTF, a CNT bundle or an individual CNT. Therefore, when an interphase is present, the interfacial stress is spread over a much larger contact area as the filler scale decreases, making the overall interface stronger. When an aligned long filler is used for reinforcement ($l \geq l_c$), a higher amount of interphase (higher penetration factor P) increases the composite strength (Supporting Information equation (S22)) yet weakens its toughness (equation (S24)), and vice versa. Here, the toughness is expressed in terms of the energy absorbed by pulling out CNTFs from the matrix during fracture [19,30,37]. Refer to the quantitative analysis in Supporting Information section S4, which uses the modified CKT model presented in the previous section, and the theoretical investigation of CNT bundles in our previous work [19].

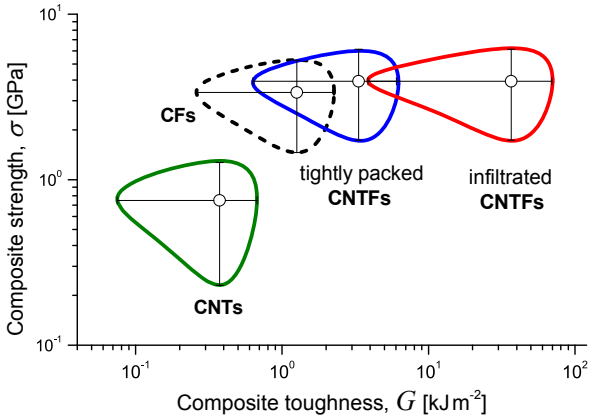

Fig. 7. Performance mapping with aligned CNTs, CNTFs and CFs reinforcement. The nanocomposite strength σ versus its toughness G, accounting only for the filler's contribution to the composite (the matrix contribution is not shown). The parameters, tolerances and calculations used in this assessment are described in Supporting Information section S4, and are based on the CNTF strength measured in the fragmentation test. The CF strength is obtained from Ref. [18]. The tolerances are depicted as ellipses (which take pear-like shapes in a log-log plot).

Additional fracture energy is absorbed by the pullout of individual CNTs or CNT bundles from the interphase, thus improving toughness. The contribution of this component scales as $G_{int}/G_{ext} \propto (\tau_{ext}/\tau_{int})^2$ (Supporting Information equation (S26)), where G is the pullout energy and the subscripts *int* and *ext* denote internal (inside the CNTF) and external (outside the CNTF), respectively. For example, by impregnating the CNTF with a softer (weaker, more ductile) matrix than the surrounding matrix, we may expect an order of magnitude improvement in toughness (assuming $\tau_{ext}/\tau_{int} \approx 3$). This finding is in agreement with observations in solution spun PVA fibers with high CNT and graphene volume fraction [38]. The improvement in toughness can be achieved with minimal impact on the overall strength, since at high volume fractions the strength is dominated by the strength of the CNT bundle. By contrast, impregnation by a hard matrix is known to increase the fiber strength [15], but will result in decreasing the toughness. The presence of an interphase may even improve the composite strength by spreading the stress more uniformly in a cross section and by arresting crack propagation.

These performance trends are summarized in Fig. 7, which maps the composite strength versus toughness for a range of the parameters, using equations (S21)-(S24) in Supporting Information section S4. The advantage of CNTF reinforcement over uniformly dispersed, aligned CNT reinforcement is evident, in both the strength and toughness, and tradeoffs between strength and toughness are possible as well. The improvement in toughness when an interphase is introduced is achieved with negligible impact on strength. By comparison, carbon fiber (CF) reinforcement is estimated to have a similar strength as CNTF reinforcement, but a much lower toughness compared to both tightly packed and infiltrated CNTFs.

4. Conclusions

A multilevel composite structure is presented, consisting of CNT fibers embedded in epoxy matrix. The proposed composite bears resemblance to a tendon as it has a similar structural hierarchy, is self-assembled from nanoscale to macroscale, and is simultaneously strong and tough, a combination rarely found in engineering materials. While such structures are common in nature, implementation difficulties impede their realization in man-made composites. By tailoring advanced experimental and theoretical techniques, we show how the degree of polymer penetration inside the CNTF can be controlled, thereby boosting the composite structural toughness and, at the same time, achieving the supreme strength owed to carbon nanotubes.

The use of CNTFs as reinforcing fillers in composites bridges the gap between nanoscale and macroscale, so perfectly realized in multi-level hierarchical biological structures. CNTFs combine the excellent mechanical properties of CNTs with the handling ease of microsized fibers. By way of surface treatment, CNTFs can be densified to a desired compactness, enabling the control of the amount of matrix penetration, an interphase, during composite preparation. The composite structure comprises four hierarchical levels from nanoscale to macroscale - individual CNTs, CNT bundles, CNTFs, and composite – allowing the tuning of the composite mechanical properties to desired strength, stiffness and toughness.

We demonstrate how the amount of interphase can be controlled by applying chemical treatments to the CNTFs. Fragmentation tests are used to characterize the strength of CNTFs in epoxy and the CNTF-epoxy interfacial strength. A highly densifying treatment, using HNO_3 as solvent, results in minimal polymer penetration into the CNTF. By contrast, a less densifying treatment, using EG as solvent, results in substantial penetration, and creation of an interphase that effectively strengthens the CNTF-matrix interface. The effective CNTF tensile and interfacial strengths, as well as the fracture behavior, are found to be greatly influenced by the amount of interphase, which is therefore key to the composite performance.

Our theoretical analysis shows that both the strength and toughness of a composite reinforced by CNTFs are potentially an order of magnitude higher than those achievable with uniformly dispersed aligned CNTs. This observation is particularly interesting and somewhat paradoxical in view of the much higher material strength of an individual CNT compared to an individual CNTF, and it echoes a general observation on natural structures in which the strength is graded from very strong components at the lowest level (nano scale) to weaker sub-structures at the higher level (micro and macro scales). Furthermore, the toughness of a CNTF reinforced composite can be increased significantly by creating an interphase, mainly because additional pullout energy is absorbed inside the CNTF, but also because an interphase helps arresting and diverting cracks propagation. The enhanced toughness seems to be a critical advantage of CNTF reinforcement over CF reinforcement. A modified (generalized) filler-failure CKT model is presented to better account for the CNTF complex internal structure including voids and interphase, amounting to about double the interfacial area in the EG treated CNTF compared to the HNO_3 treated CNTF.

These preliminary results should be expanded in future research by exploring additional methods for tuning the interphase, so as to clarify the role of matrix penetration in the composite mechanical performance. Such tuning could be done by, for example, using polymer solutions with different viscosities, impregnating CNTFs with a softer polymer, treating CNTFs to achieve various levels of density, and applying different vacuum/temperature/time conditions to control the penetration process. Further exploration should also address implementation of CNTF based composites in applications requiring strong and tough structures, as well as in bioengineering.

Acknowledgements

The authors would like to acknowledge partial support from the INNI Focal Technology Area program “Inorganic nanotubes (INT): from nanomechanics to improved nanocomposites”, the G.M.J. Schmidt Minerva Centre of Supramolecular Architectures at the

Weizmann Institute, and the China-Israel Science Foundations collaborative research grant. This research was also made possible in part by the generosity of the Harold Perlman family. H.D.W. is the recipient of the Livio Norzi Professorial Chair in Materials Science.

Appendix A. Supplementary data

Supplementary data related to this article can be found at http://dx.doi.org/10.1016/j.compscitech.2016.10.011.

References

[1] S. Weiner, H.D. Wagner, The material bone: structure mechanical function relations, Annu. Rev. Mater Sci. 28 (1998) 271–298.
[2] K. Autumn, Y.A. Liang, S.T. Hsieh, W. Zesch, W.P. Chan, T.W. Kenny, R. Fearing, R.J. Full, Adhesive force of a single gecko foot-hair, Nature 405 (6787) (2000) 681–685.
[3] H.J. Ensikat, P. Ditsche-Kuru, C. Neinhuis, W. Barthlott, Superhydrophobicity in perfection: the outstanding properties of the lotus leaf, Beilstein J. Nanotechnol. 2 (2011) 152–161.
[4] S. Iijima, Helical microtubules of graphitic carbon, Nature 354 (1991) 56–58.
[5] J.N. Coleman, U. Khan, W.J. Blau, Y.K. Gun'ko, Small but strong: a review of the mechanical properties of carbon nanotube-polymer composites, Carbon 44 (9) (2006) 1624–1652.
[6] W.B. Lu, M. Zu, J.H. Byun, B.S. Kim, T.W. Chou, State of the art of carbon nanotube fibers: opportunities and challenges, Adv. Mater 24 (14) (2012) 1805–1833.
[7] Y.L. Li, I.A. Kinloch, A.H. Windle, Direct spinning of carbon nanotube fibers from chemical vapor deposition synthesis, Science 304 (5668) (2004) 276–278.
[8] K.L. Jiang, Q.Q. Li, S.S. Fan, Nanotechnology: spinning continuous carbon nanotube yarns - carbon nanotubes weave their way into a range of imaginative macroscopic applications, Nature 419 (6909) (2002), 801–801.
[9] B. Vigolo, A. Penicaud, C. Coulon, C. Sauder, R. Pailler, C. Journet, P. Bernier, P. Poulin, Macroscopic fibers and ribbons of oriented carbon nanotubes, Science 290 (5495) (2000) 1331–1334.
[10] K. Koziol, J. Vilatela, A. Moisala, M. Motta, P. Cunniff, M. Sennett, A. Windle, High-performance carbon nanotube fiber, Science 318 (5858) (2007) 1892–1895.
[11] G. Xu, J. Zhao, S. Li, X. Zhang, Z. Yong, Q. Li, Continuous electrodeposition for lightweight, highly conducting and strong carbon nanotube-copper composite fibers, Nanoscale 3 (10) (2011) 4215–4219.
[12] H.D. Espinosa, T. Filleter, M. Naraghi, Multiscale experimental mechanics of hierarchical carbon-based materials, Adv. Mater 24 (21) (2012) 2805–2823.
[13] J.J. Vilatela, R. Khare, A.H. Windle, The hierarchical structure and properties of multifunctional carbon nanotube fibre composites, Carbon 50 (3) (2012) 1227–1234.
[14] Y. Jung, T. Kim, C.R. Park, Effect of polymer infiltration on structure and properties of carbon nanotube yarns, Carbon 88 (2015) 60–69.
[15] Y.N. Liu, M. Li, Y.Z. Gu, X.H. Zhang, J.N. Zhao, Q.W. Li, Z.G. Zhang, The interfacial strength and fracture characteristics of ethanol and polymer modified carbon nanotube fibers in their epoxy composites, Carbon 52 (2013) 550–558.
[16] H.D. Wagner, A. Eitan, Interpretation of the fragmentation phenomenon in single-filament composite experiments, Appl. Phys. Lett. 56 (20) (1990) 1965–1967.
[17] B. Yavin, H.E. Gallis, J. Scherf, A. Eitan, H.D. Wagner, Continuous monitoring of the fragmentation phenomenon in single fiber composite materials, Polym. Compos 12 (6) (1991) 436–446.
[18] N. Lachman, B.J. Carey, D.P. Hashim, P.M. Ajayan, H.D. Wagner, Application of continuously-monitored single fiber fragmentation tests to carbon nanotube/carbon microfiber hybrid composites, Comp. Sci. Technol. 72 (14) (2012) 1711–1717.
[19] I. Greenfeld, H.D. Wagner, Nanocomposite toughness, strength and stiffness -the role of filler geometry, Nanocomposites 1 (1) (2014) 3–17.
[20] S. Li, X. Zhang, J. Zhao, F. Meng, G. Xu, Z. Yong, J. Jia, Z. Zhang, Q. Li, Enhancement of carbon nanotube fibres using different solvents and polymers, Compos. Sci. Technol. 72 (12) (2012) 1402–1407.
[21] F. Meng, J. Zhao, Y. Ye, X. Zhang, Q. Li, Carbon nanotube fibers for electrochemical applications: effect of enhanced interfaces by an acid treatment, Nanoscale 4 (23) (2012) 7464–7468.
[22] J. Jia, J. Zhao, G. Xu, J. Di, Z. Yong, Y. Tao, C. Fang, Z. Zhang, X. Zhang, L. Zheng, Q. Li, A comparison of the mechanical properties of fibers spun from different carbon nanotubes, Carbon 49 (4) (2011) 1333–1339.
[23] J.T. Di, Z.Z. Yong, X.J. Yang, Q.W. Li, Structural and morphological dependence of carbon nanotube arrays on catalyst aggregation, Appl. Surf. Sci. 258 (1) (2011) 13–18.
[24] L.S. Schadler, S.C. Giannaris, P.M. Ajayan, Load transfer in carbon nanotube epoxy composites, Appl. Phys. Lett. 73 (26) (1998) 3842–3844.
[25] K. Wang, M. Li, Y.N. Liu, Y.Z. Gu, Q.W. Li, Z.G. Zhang, Effect of acidification conditions on the properties of carbon nanotube fibers, Appl. Surf. Sci. 292 (2014) 469–474.
[26] S. Li, X. Zhang, J. Zhao, F. Meng, G. Xu, Z. Yong, J. Jia, Z. Zhang, Q. Li, Enhancement of carbon nanotube fibres using different solvents and polymers, Compos. Sci. Technol. 72 (12) (2012) 1402–1407.
[27] Z.Q. Zhang, B. Liu, Y.L. Chen, H. Jiang, K.C. Hwang, Y. Huang, Mechanical properties of functionalized carbon nanotubes, Nanotechnology 19 (39) (2008).
[28] Hexion, 2005. http://www.silmid.com/MetaFiles/Silmid/13/13ad44ed-5d5d-41e2-84a3-351dfdf5b30f.pdf.
[29] A.H. Cottrell, Strong solids, Proc. R. Soc. Lond. A 282 (1964) 2–9.
[30] A. Kelly, W.R. Tyson, Tensile properties of fibre-reinforced metals - copper/tungsten and copper/molybdenum, J. Mech. Phys. Solids 13 (1965) 329–350.
[31] M. Zu, Q. Li, Y. Zhu, M. Dey, G. Wang, W. Lu, J.M. Deitzel, J.W. Gillespie Jr., J.-H. Byun, T.-W. Chou, The effective interfacial shear strength of carbon nanotube fibers in an epoxy matrix characterized by a microdroplet test, Carbon 50 (3) (2012) 1271–1279.
[32] F. Deng, W. Lu, H. Zhao, Y. Zhu, B.-S. Kim, T.-W. Chou, The properties of dry-spun carbon nanotube fibers and their interfacial shear strength in an epoxy composite, Carbon 49 (5) (2011) 1752–1757.
[33] A.H. Barber, R. Andrews, L.S. Schadler, H.D. Wagner, On the tensile strength distribution of multiwalled carbon nanotubes, Appl. Phys. Lett. 87 (20) (2005) 203106.
[34] H.D. Wagner, J. Aronhime, G. Marom, Dependence of the tensile-strength of pitch-based carbon and para-aramid fibers on the rate of strain, P Roy. Soc. Lond a Mat. 428 (1875) (1990) 493–510.
[35] J. Kastelic, A. Galeski, E. Baer, Multicomposite structure of tendon, Connect. Tissue Res. 6 (1) (1978) 11–23.
[36] U. Akiva, H.D. Wagner, S. Weiner, Modelling the three-dimensional elastic constants of parallel-fibred and lamellar bone, J. Mater. Sci. 33 (6) (1998) 1497–1509.
[37] M. Piggott, Load Bearing Fibre Composites, second ed., Kluwer Academic Publishers2002.
[38] M.K. Shin, B. Lee, S.H. Kim, J.A. Lee, G.M. Spinks, S. Gambhir, G.G. Wallace, M.E. Kozlov, R.H. Baughman, S.J. Kim, Synergistic toughening of composite fibres by self-alignment of reduced graphene oxide and carbon nanotubes, Nat. Commun. 3 (2012).